# An Analytical Approach to Design of Ultrasonic Transducers Considering Lateral Vibrations

## M.R. Karafi*, S.A. Mirshabani

Mechanical Engineering Department, Tarbiat Modares University, Tehran, Iran.

## Article info

## Abstract

The purpose of this paper is to develop a design procedure for Langevin ultrasonic transducers with lateral dimensions larger than a quarter of the longitudinal wave length. In this case, the assumption of the one-dimensional design is not valid, and this method cannot predict the experimental resonance frequency. Some researchers have considered radial and longitudinal normal stresses by means of the apparent elasticity method and reduced the error between the design and experimental resonance frequency. In this research, 3D normal stresses of a transducer's components i.e. longitudinal, radial and circumferential were considered in the design procedure. The apparent elasticity method was used to modify the elastic modulus and the wave numbers of the transducer's components. Resonance lengths of the components were then calculated using the modified values. The design resonance frequency of the transducer was 20kHz. The experimental resonance frequency was measured as 19810Hz. The error of 0.95% between analytical and experimental results showed that the new design procedure can fairly estimate the resonance frequency of the transducer.

## Nomenclature

| | | | |
|---|---|---|---|
| $A_i$ | Cross section area of the ith part of the transducer | $F_i$ | Boundary force of the ith part of the trasducer |
| $A, B, C, D$ $E, F, G$ $H, I, J, M$ $N, O, Q$ | Longitudenal vibration amplitude coeficients | $E_i$ | Apparent young modulus of the ith part of the transducer (in z direction) |
| | | $c_{ij}^E$ | Elasticity tensor of the piezoelectric at the constant electric field |
| $C_1, C_2$ | Radial vibration amplitude coeficients | $b$ | Inner radious of a hollow cylinder |
| $T_r, T_z, T_\theta$ | Normal stresses in the piezoelectric | $t$ | Time |
| $J(x), y(x)$ | Functions to simplify equations | $a$ | Outer radius of a hollow cylinder |
| $J_1, Y_1, J_0, Y_0$ | Bessel functions | $e_{ij}$ | Piezoelectric stress tensor |
| $k_i$ | Apparent longitudinal wave number of the ith part of the transducer | $S_{ij}^E$ | Compliance tensor of the piezoelectric the at constant electric field |
| $E_z$ | Apparent young modulus in z direction | $E_r$ | Apparent young modulus in r direction |

| | | | |
|---|---|---|---|
| $E$ | Real young modulus | $\sigma_\theta$ | Normal circumferential stress |
| $S_\theta$ | Circumferential strain | $k_z$ | Apparent wave number along z direction |
| $k_r$ | Apparent wave number along radial direction | $l_i$ | Length of the i$^{\text{th}}$ part of the transducer |
| $n_i$ | Mechanical coupling coefficient of the i$^{\text{th}}$ part of the transducer | $z_i$ | Local z coordinate of the i$^{\text{th}}$ part of the transducer |
| $S_z$ | Longitudinal strain | $S_r$ | Radial strain |
| $u_r$ | Radial displacement | $u_z$ | Longitudinal displacement |
| $u_i$ | Longitudinal displacement of the i$^{\text{th}}$ part of the transducer | $\varepsilon_{ij}^T$ | Relative permittivity tensor of the piezoelectric |
| $r$ | r Coordinate | $V_r$ | Apparent sound velocity along r direction |
| $w$ | Angular frequency | $\nu$ | Poison ratio |
| $\rho$ | Density | $V_z$ | Apparent sound velocity along z direction |
| $\sigma_z$ | Normal longitudinal stress | $\sigma_r$ | Normal radial stress |

# 1. Introduction

The purpose of this research is to develop a design procedure for Langevin ultrasonic transducers with lateral dimensions larger than a quarter of the longitudinal wave length. Bolt-clamped Langevin transducers are widely used in various applications such as cleaning, plastic and metal welding, machining processes, metal forming, polymers production processes, wastewater treatment, under-water communication and other industrial applications [1-6]. Widespread use of this kind of transducers reflects the necessity of an analytical method to design these transducers. These transducers consist of some piezoelectric rings which are sandwiched by two metal parts. Typically, the backing part is a stainless steel hollow cylinder; the matching part is aluminum or titanium solid cylinder with a threated hole. A screw bolt is used to clamp all the parts. In conventional design methods, transducers are assumed to vibrate longitudinally, and lateral vibrations are neglected [7]. Generally speaking, when the lateral dimensions are less than a quarter of the longitudinal wavelength, one-dimensional design method can be used and the error between the measured and designed frequency is not significant. In the case of transducers which have lateral dimensions larger than a quarter of wave length, the transducer has a coupled vibration consisting of longitudinal and lateral vibrations. Therefore, a new design theory is needed to study the vibrational behavior of the transducers. To study the coupled vibrations of ultrasonic transducers, FEM methods are usually used [8-9]. But analytical methods are preferred because of the deep insight they provide about physical parameters of the system. Mori et al introduced the apparent elasticity method [10] and used it to study high power ultrasonic radiators of thick plates and short column [11-12]. Based on the method presented by Mori, the coupled vibrations of piezoelectric, radiators, and transducers have been studied in some researches. Shuyu applied the method for designing an ultrasonic transducer which consisted of metal end parts with rectangular cross-section and two piezoelectric rings [13]. Due to excitation of complex modes, rectangular cross-section parts for head and tail mass are not common for ultrasonic transducers. Therefore, frequency equations of this research are not applicable for circular cross-section transducers. In addition, in this paper radial and circumferential normal stresses of piezoelectric elements are assumed equal. And also the effect of the central bolt is neglected. Dragan, Milan, Liang and Zhou applied the apparent elasticity method to design transducers [14-15]. In these two researches, the mechanical coupling coefficient was defined as the ratio of the longitudinal stress to the radial stress. It was also assumed that the radial stress was equal to the circumferential stress. Shuyu studied coupled vibrations of a piezoelectric disk resonator, and a metal hollow cylinder separately using apparent elasticity method [16-17].

In this paper, a design procedure of ultrasonic transducers is developed based on apparent elasticity method. The procedure considers 3D normal stresses of transducers' components. Mechanical coupling coefficient was defined as the ratio of longitudinal normal stress to lateral normal stresses i.e. radial and circumferential normal stresses. The procedure was applied to design a commercial ultrasonic transducer. Mechanical coupling coefficient of each part was achieved at the design resonance frequency. Then the elastic modulus and wave numbers of the components were modified. After that, using the longitudinal frequency equation of the transducer, the resonance lengths of the transducer's components were calculated. The designed transducers with the one-dimensional and the new method were simulated using ANSYS software and their resonance frequencies were compared with the analytical one. Ultimately, the transducer which designed with the new method was manufactured and the experimental resonance frequency is compared with the analytical counterpart. The results showed that the new method can fairly predict the experimental resonance frequency.

## 2. Design Procedure

Some parameters should be determined as input values of the design procedure. These parameters are resonance frequency, nominal power, mode shape, node position, and material physical properties of components. The resonance frequency of ultrasonic transducers should be chosen above 20kHz to be out of the human audible frequency range. The higher the resonance frequency is, the lower the wave length will be. The length of the transducer should be half of the wavelength to generate the resonant standing wave. In this research, the design resonance frequency was 20kHz. The intended output power is the key factor for selection of the number, size and type of piezoelectric rings required. The nominal power of the transducer was chosen as 300W. The maximum allowable power delivered by each piece of piezoelectric ring depends on the quality, treatment, production processes and its dimensions. This power is commonly said to range from 15 to 30W/cm² [7]. Piezoelectric rings are available in standard sizes in markets. Therefore, two piezoelectric ceramic ring of the type PZT4 (Lead Zirconate Titanate) were used. The power per area and the size of the piezoelectric rings are stated in Table 1. Further, mode shape and nodes position of the transducer should be determined in the design procedure. First longitudinal mode shape of the transducer was chosen, because the stiffness of the first mode is lower than that of the next modes and its excitation is easier. The first longitudinal mode has one node. As the matching part has more strength than the piezoelectric ceramics, this is the best place to locate the node. The flange area of the matching is an appropriate place to clamp the transducers to housings or other equipment. To achieve maximum transmission of ultrasound between the piezoelectric and medium, the matching part is usually made up of aluminum or titanium [7]. Heat conduction and machinability of the aluminum are more than those of titanium, but mechanical and corrosion strength of titanium is more than aluminum's. The backing is recommended to be made up of steel to reduce vibrations at the end of the transducer. Stainless steel 303 or 304 are suggested for backing, and aluminum 7075-T6 for matching materials with regard to acoustic properties and acceptable performance in practice. Based on what has already been discussed, the specifications and material physical properties of the transducer are expressed in Tables 1 and 2.

### 2.1. Assumptions of the Design Procedure

- Lateral dimensions of the transducer are not necessary to be less than a quarter of the sound wave length.

- Lateral vibrations toward radial and circumferential direction are not negligible.

- Lateral stresses along radial and circumferential direction are not necessarily equal.

- Longitudinal and lateral vibrations are sinusoidal.

- Diameter variation along the transducer is far enough from critical value. Meanwhile, the influence of fillet and chamfers in the corners is ignored.

- Acoustic impedance of air is considered to be zero; so that a transducer that operates in air is called unloaded transducer.

- Copper electrodes are considered to be of the same material as piezoelectric rings.

- Two piezoelectric rings and two copper electrodes are considered as one integrated part.

- Flat surfaces on the backing and matching which are machined to ease the assembly are ignored.

Fig. 1 demonstrates the mode shape, node position, main components, and the boundary conditions of the transducer.

**Table 1**
Specifications of the transducer.

| Parameter | Value |
| --- | --- |
| Design resonance frequency | 20000Hz |
| Vibration mode | First longitudinal mode |
| Position of node | On the matching step |
| Matching material | Aluminum 7075-T6 |
| Backing material | Stainless steel 304 |
| Piezoelectric dimensions | External diameter 50mm Internal diameter 20mm Thickness 6mm |
| Number of piezoelectric | 2 rings |
| Thickness of copper electrodes | 0.5mm |
| Piezoelectric type | PZT4 |
| Power per unit area of the piezoelectric | 18W/cm² |
| Nominal power of the transducer | 300W |

**Table 2**
Physical properties of the transducer's components.

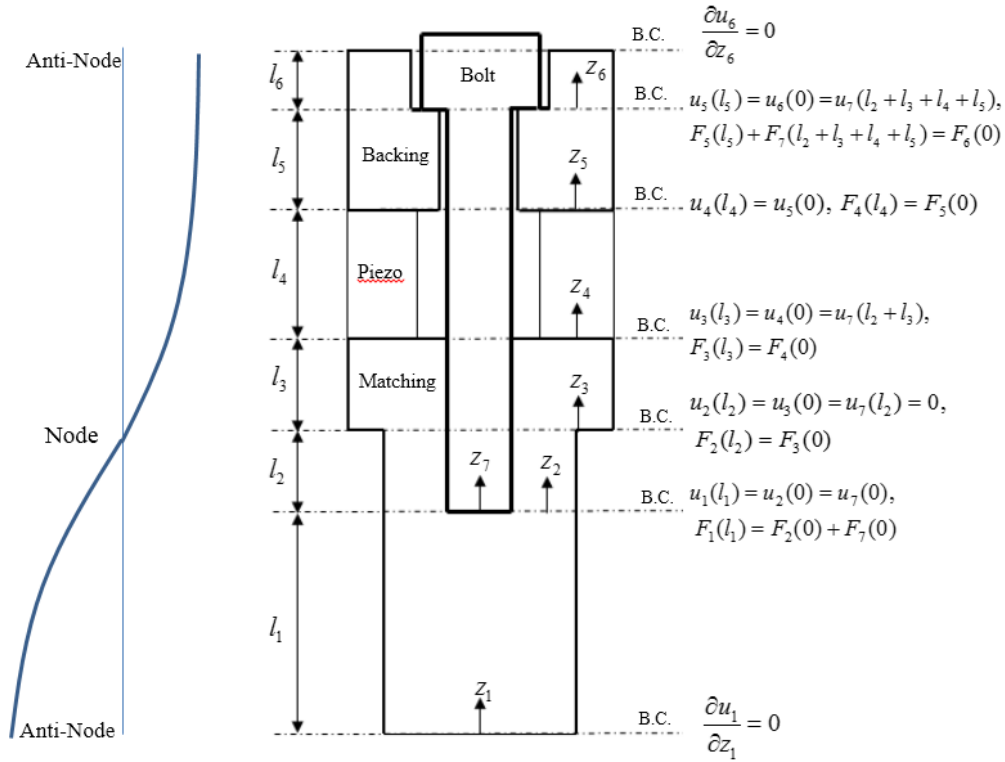| Material | Poisson ratio | Real elasticity module(GPa) | Density |
| --- | --- | --- | --- |
| Aluminum 7075-T6 | 0.33 | 73 | 2823 |
| Stainless steel 304 | 0.28 | 200.57 | 7917 |
| Piezoelectric PZT4 | 0.3 | 115.41 (in "33" direction) | 7500 |

**Fig. 1.** Mode shape, node position, main components and boundary conditions of the transducer.

Differential equations of longitudinal vibrations of the transducer's components are the same as Eq. (A13). Analytical solution of the equation for each component is as follows:

$$u_1(z_1) = A \cos k_1 z_1 + B \sin k_1 z_1 \tag{1}$$

$$u_2(z_2) = C \cos k_2 z_2 + D \sin k_2 z_2 \tag{2}$$

$$u_3(z_3) = E \cos k_3 z_3 + F \sin k_3 z_3 \tag{3}$$

$$u_4(z_4) = G \cos k_4 z_4 + H \sin k_4 z_4 \tag{4}$$

$$u_5(z_5) = I \cos k_5 z_5 + J \sin k_5 z_5 \tag{5}$$

$$u_6(z_6) = M \cos k_6 z_6 + N \sin k_6 z_6 \tag{6}$$

$$u_7(z_7) = P \cos k_7 z_7 + Q \sin k_7 z_7 \tag{7}$$

where, A, B, C, D, E, F, G, H, I, J, M, N, P, and Q are constants which can be obtained by the boundary conditions of Fig. 1.

$$B = E = 0 \tag{8}$$

$$C = P = A \cos k_1 l_1 \tag{9}$$

$$Q = -A \frac{\cos k_1 l_1 \cos k_7 l_2}{\sin k_7 l_2} \tag{10}$$

$$D = A \left( -\frac{A_1 E_1 k_1 \sin k_1 l_1}{A_2 E_2 k_2} + \frac{A_7 E_7 k_7 \cos k_1 l_1 \cos k_7 l_2}{A_2 E_2 k_2} \right) \tag{11}$$

$$F = -C \frac{A_2 E_2 k_2 \sin k_2 l_2}{A_3 E_3 k_3} + D \frac{A_2 E_2 k_2 \cos k_2 l_2}{A_3 E_3 k_3} \tag{12}$$

$$G = F \sin k_3 l_3 \tag{13}$$

$$H = F \frac{A_3 E_3 k_3 \cos k_3 l_3}{A_4 E_4 k_4} \tag{14}$$

$$I = G \cos k_4 l_4 + H \sin k_4 l_4 \tag{15}$$

$$J = -G \frac{A_4 E_4 k_4 \sin k_4 l_4}{A_5 E_5 k_5} + H \frac{A_4 E_4 k_4 \cos k_4 l_4}{A_5 E_5 k_5} \tag{16}$$

$$M = I \cos k_5 l_5 + J \sin k_5 l_5 \tag{17}$$

$$N = -I \frac{A_5 E_5 k_5 \sin k_5 l_5}{A_6 E_6 k_6} + J \frac{A_5 E_5 k_5 \cos k_5 l_5}{A_6 E_6 k_6}$$

$$- P \frac{A_7 E_7 k_7 \sin k_7 (l_2 + l_3 + l_4 + l_5)}{A_6 E_6 k_6}$$

$$+ Q \frac{A_7 E_7 k_7 \cos k_7 (l_2 + l_3 + l_4 + l_5)}{A_6 E_6 k_6} \tag{18}$$

The frequency equations of the longitudinal vibrations of the transducer are as follows:

$$C \cos k_2 l_2 + D \sin k_2 l_2 = 0 \qquad (19)$$

$$- M \cos k_6 l_6 + N \sin k_6 l_6 = 0 \qquad (20)$$

where $u_i$, $z_i$, $k_i$, $A_i$, and $E_i$ are longitudinal displacement, longitudinal coordinate, apparent longitudinal wave number, cross-section area, and apparent longitudinal elastic modulus of the $i^{\text{th}}$ part, respectively. The design procedure of the transducer consists of the following steps:

**Step 1:** Using radial frequency equations of the transducer's parts, the mechanical coupling coefficient of each part is calculated at the design resonance frequency, with known lateral dimensions and physical properties.

**Step 2:** the Elastic modulus and wave number of each part are modified using its mechanical coupling coefficient.

**Step 3:** Using the modified values as well as the transducer longitudinal frequency Eqs. (19) and (20), it is possible to calculate the components resonance lengths.

Since the boundary conditions of the transducer radial vibrations are the same as those of a free cylinder, it is possible to use radial frequency equations of a free cylinder for the transducer. According to Fig.1, the first and seventh parts of the transducer are solid cylinders. Therefore, the radial frequency equation of a solid cylinder (Eq. (A24)) was used to calculate the mechanical coupling coefficients. The apparent radial wave number in this equation is as follows:

$$k_r = \frac{w}{\sqrt{\dfrac{E(2 - \nu n)}{\rho(1 + \nu)(1 - \nu - 2\nu n)}}} \qquad (21)$$

where $w$, $n$, $\nu$ and are angular frequency, mechanical coupling coefficient, Poisson's ratio, and real elastic modulus of each part of the transducer. The apparent radial wave number at the frequency of 20kHz is substituted in the Eq. (A24). In this equation, dimensions, physical properties and the resonance frequency were known. Therefore, the mechanical coupling coefficient was calculated numerically using Maple software. The calculated values were used to obtain the apparent longitudinal wave number and apparent elastic modulus of the two parts using Eqs. (A10 and A12).

Parts 2, 3, 5, and 6 in Fig. 1 are hollow cylinders. Therefore, radial frequency equation of a free hollow cylinder, Eq. (A23), was used to calculate the mechanical coupling coefficient of these parts the same as what discussed for the parts 1 and 7. The radial frequency equation of a piezoelectric ring, Eq. (A39), was used to calculate the mechanical coupling coefficient of the piezoelectric. Finally, Eqs. (A41 and A42) were used to calculate the apparent longitudinal wave number and elastic modulus of the piezoelectric. Table 3 shows the mechanical coupling coefficients, real and apparent elastic modulus and wave number of each part of the transducer.

Two frequency Eqs. of (19) and (20) were used to calculate the resonance lengths of the transducer. Some lengths should be determined first. $l_4 = 2l_{\text{piezo}} + 2l_{\text{electrod}} = 13mm$ was the length of the piezoelectric rings which consisted of the thickness of two piezoelectric rings and two copper electrodes. $l_6$ was selected as 8mm to embed the head of the bolt in the backing part. Using frequency Eq. (19) and determining one the lengths of $l_2$ or $l_1$, it is possible to calculate the other length. Furthermore, Using frequency Eq. (20) and determining one of the lengths of $l_3$ or $l_5$, it is possible to calculate the other length. It must be taken into account that the total length of the transducer is near the mean half wavelengths of the components. In the procedure, $l_2$ and $l_3$ were selected as 15mm and 8mm respectively. $l_1$ and $l_5$ were calculated using the longitudinal frequency equations. Table 4 compares the resonance lengths of the transducer which were calculated by the one-dimensional and the apparent elasticity method.

**Table 3**
The mechanical coupling coefficient, elastic modulus and wave number of each section of the transducer.

| i Part number | E (Gpa) Real elastic modulus | k (rad/m) Real wave number | $n_i$ Mechanical coupling coefficient | $E_i$(GPa) Apparent elastic modulus | $k_i$ (rad/m) Apparent wave number |
|---|---|---|---|---|---|
| 1 | 73 | 24.71 | -23.17 | 71.97 | 24.88 |
| 2 | 73 | 24.71 | -37.4 | 72.36 | 24.82 |
| 3 | 73 | 24.71 | -19.26 | 71.77 | 24.92 |
| 4 | 115.41 | 32.03 | -2.64 | 57.1 | 45.54 |
| 5 | 200.57 | 24.96 | -20.1 | 197.81 | 25.13 |
| 6 | 200.57 | 24.96 | -15.8 | 197.07 | 25.18 |
| 7 | 200 | 24.81 | -320.1 | 199.82 | 24.82 |

**Table 4**
Dimensions of the transducer designed by the one-dimensional and apparent elasticity methods.

| $i^{th}$ part number | External radius (mm) | Internal radius (mm) | Length (mm) | One-dimensional method | Apparent elasticity method |
|---|---|---|---|---|---|
| 1 | 20 | 0 | $l_1$ | 50.5 | 50 |
| 2 | 20 | 6 | $l_2$ | 15 | 15 |
| 3 | 25 | 6 | $l_3$ | 8 | 8 |
| 4 | 25 | 10 | $l_4$ | 13 | 13 |
| 5 | 25 | 6.5 | $l_5$ | 21.1 | 12.7 |
| 6 | 25 | 11 | $l_6$ | 8 | 8 |
| 7 | 6 | 0 | $l_7 = l_2 + l_3 + l_4 + l_5$ | 57.1 | 48.7 |

## 3. FEM Analysis of the Transducer

Finite element modal analysis of the transducer was performed using ANSYS software. SOLID 186 elements were used to mesh the matching, backing and the bolt, and SOLID 227 was used for the piezoelectric rings. Compliance tensor at the constant electric field $[s_{ij}^E]$, elasticity tensor at constant electric field $[c_{ij}^E]$, piezoelectric stress tensor $[e_{ij}]$ and the relative permittivity tensor at constant stress $[\varepsilon_{ij}^T]$ of the PZT4 are as follows [18]:

$$[s_{ij}^E] =$$

$$\begin{bmatrix} 12.3 & -4.05 & -5.31 & 0 & 0 & 0 \\ -4.05 & 12.3 & -5.31 & 0 & 0 & 0 \\ -5.31 & -5.31 & 15.5 & 0 & 0 & 0 \\ 0 & 0 & 0 & 39 & 0 & 0 \\ 0 & 0 & 0 & 0 & 39 & 0 \\ 0 & 0 & 0 & 0 & 0 & 32.7 \end{bmatrix} \times 10^{-12} m^2/N$$

$$[c_{ij}^E] = [s_{ij}^E]^{-1} =$$

$$\begin{bmatrix} 1.389 & 0.778 & 0.742 & 0 & 0 & 0 \\ 0.778 & 1.389 & 0.742 & 0 & 0 & 0 \\ 0.742 & 0.742 & 1.154 & 0 & 0 & 0 \\ 0 & 0 & 0 & 0.256 & 0 & 0 \\ 0 & 0 & 0 & 0 & 0.256 & 0 \\ 0 & 0 & 0 & 0 & 0 & 0.305 \end{bmatrix} \times 10^{11} N/m^2$$

$$[e_{ij}] = \begin{bmatrix} 0 & 0 & -4.1 \\ 0 & 0 & -4.1 \\ 0 & 0 & 14.1 \\ 0 & 0 & 0 \\ 0 & 10.5 & 0 \\ 10.5 & 0 & 0 \end{bmatrix} \frac{C}{m^2}$$

$$[\varepsilon_{ij}^T] = \begin{bmatrix} 1475 & 0 & 0 \\ 0 & 1475 & 0 \\ 0 & 0 & 1300 \end{bmatrix}$$

The electrical properties of the piezoelectric ring should be inserted to the software to apply the boundary condition of constant electrical field. The transducer which was designed by the one-dimensional and the new method was modeled and analyzed using ANSYS software. The number of elements was 35078. The modal analyses were done at free mechanical conditions. Piezoelectric electrodes were connected to ground electrical potential. The dielectric loss factor of the piezoelectric was entered to the software as $n\delta = 0.00132$. Figs. 2 and 3 show the results of the simulations.
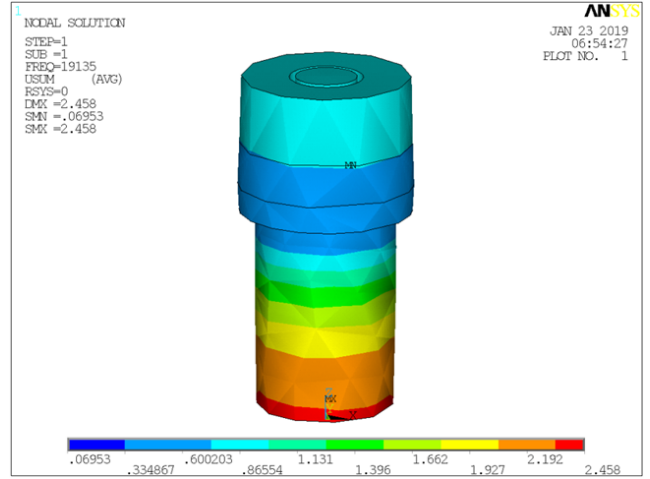


**Fig. 2.** Modal analysis of the designed transducer using the apparent elasticity method.

Fig. 2 shows that the first longitudinal mode shape of the transducer whose design used the apparent elasticity method. The resonance frequency was 19135Hz. There is the error of 4.3% between the design resonance frequency and the numerical simulation.

Fig. 3 shows that the first longitudinal mode shape of the transducer whose design used the one-dimensional method. The resonance frequency was 18054Hz. There is the error of 9.7% between the design resonance frequency and the numerical simulation.

## 4. Experimental Tests

The transducer which was designed with the new method is shown in Fig. 4, indicating the transducer and its components. The transducer was excited by an ultrasonic power supply with a square bipolar signal of 500V zero to peak, 5A zero to peak currents and the frequency range of 15kHz through 40kHz. Voltage amplitude was kept constant, and the frequency was swept near the predicted resonance frequency. The electrical impedance of the transducer decreased at the resonance frequency. Consequently, maximum electrical current was consumed at this frequency. This behavior was used to find the resonance frequency of the transducer.

The mechanical preload of the transducer which

was applied with the central bolt was 34MPa [7]. Heat glues were used to damp the vibrations of the electrodes. The melting point of the glue was 85 Co and its thickness was about 1 cm. Experimental resonance frequency of the transducer was measured as 19810Hz. Fig. 5 shows the experimental setup of measuring the radial and longitudinal vibration amplitudes of the head of the transducer.

The displacements of the head of the transducer were measured by an eddy current gap-sensor, Model AEC-5509 manufactured by Applied Electronics Corp, Japan. The conversion ratio of the sensor was 0.4mm/V. Table 5 summarizes the analytical, numerical, and experimental results of the transducer.
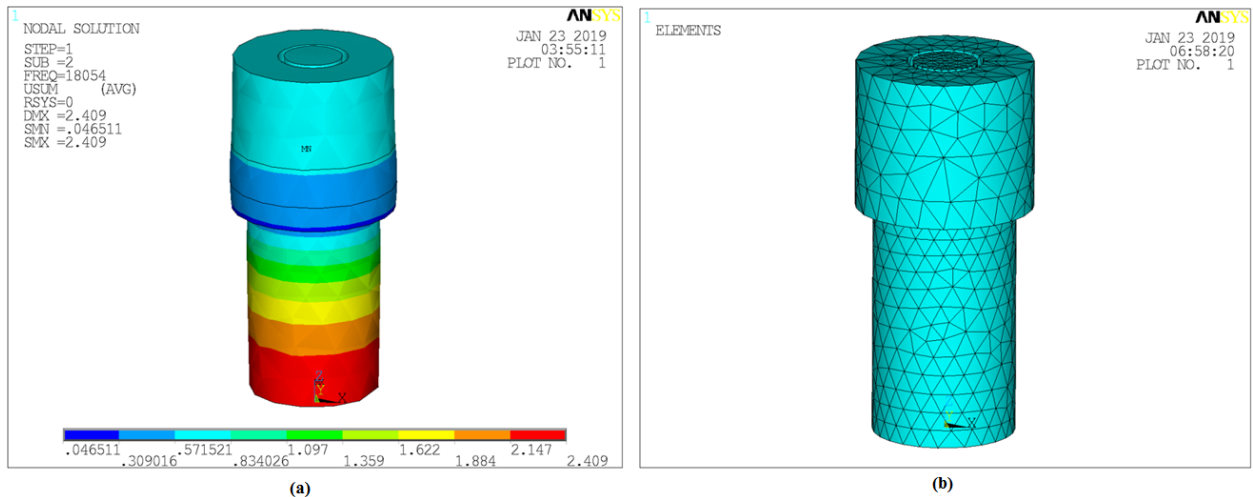


**Fig. 3.** a) Modal analysis of the designed transducer using the one-dimensional method, b) Meshed model of the transducer.
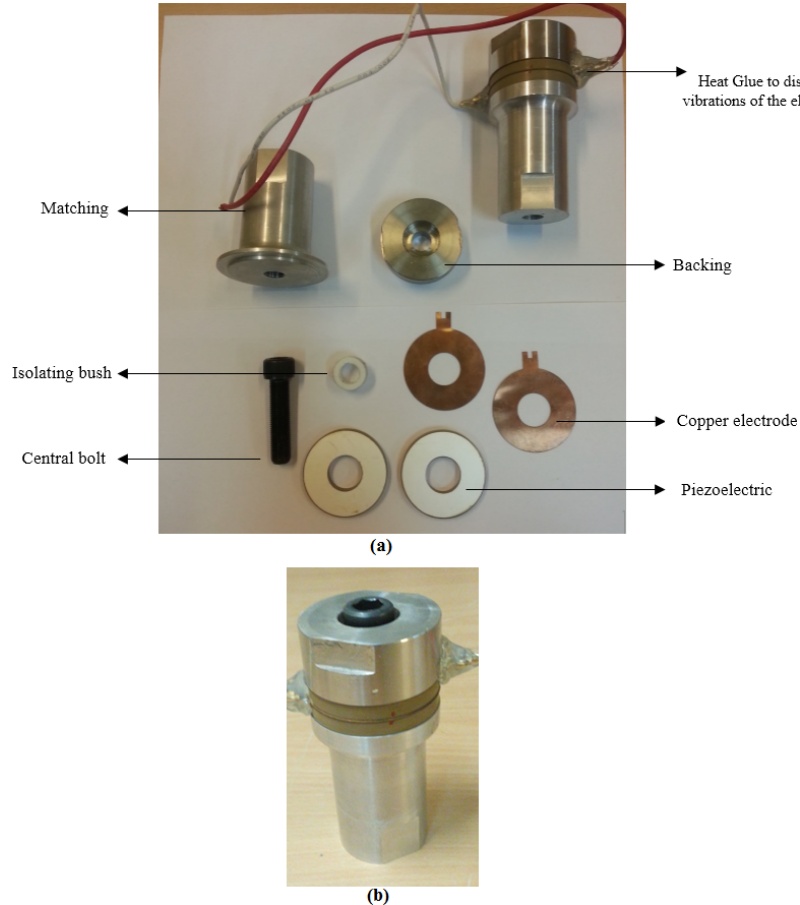


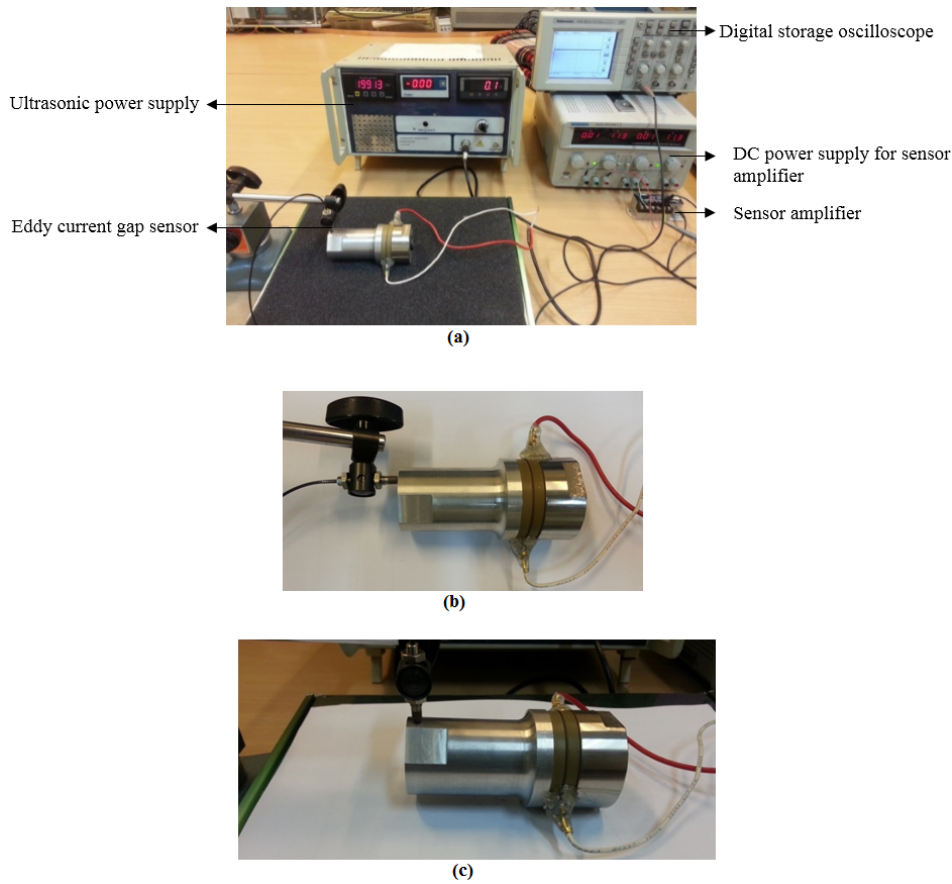**Fig. 4.** a) Transducer's components, b) Assembled transducer.

**Fig. 5.** a) Experimental setup of measuring displacements, b) Longitudinal displacement measurement, c) Radial displacement measurement.

**Table 5**
Comparison of the analytical, numerical and experimental results.

| Parameter | Value |
| --- | --- |
| Design resonance frequency of the transducer | 20000Hz |
| Numerical resonance frequency of the transducer designed by the one-dimensional method | 18054Hz |
| Numerical resonance frequency of the transducer designed by the new method | 19135Hz |
| Experimental resonance frequency of the transducer designed by the new method | 19810Hz |
| Radial displacement of the head of the transducer | 18 micrometer |
| Longitudinal displacement of the head of the transducer | 35 micrometer |
| Error between the numerical resonance frequency of the transducer designed by the one-dimensional method with the design resonance frequency | 9.7% |
| Error between the numerical resonance frequency of the transducer designed by the new method with the design resonance frequency | 4.3% |
| Error between the experimental resonance frequency with the numerical resonance frequency of the transducer designed by the new method | 3.4% |
| Error between the experimental resonance frequency with the design resonance frequency | 0.95% |

## 5. Conclusions

In this paper, a new design procedure for Langevin ultrasonic transducers was developed based on apparent elasticity method. In this method, the effect of lateral vibrations including both radial and circumferential is taken into account with the definition of the mechanical coupling coefficient. The mechanical coupling coefficient of each part was calculated. The calculated coefficient was used to modify the wave number and elastic modulus of each part. The modified parameters were used to calculate resonance lengths of the components. The designed transducers were modeled and analyzed numerically by ANSYS software. The transducer designed by the apparent elasticity method was fabricated and its resonance frequency was compared with theoretical and numerical one. Also, radial and

longitudinal displacements were measured experimentally. The error between the theoretical and experimental resonance frequency was 0.95%. The results indicated that the new design method can fairly predict the resonance frequency of the transducer.

## Appendix A

### A.1. Theoretical Equations of the Transducer Vibrations

A cylindrical element was considered for the analytical modeling. All stresses exerted on the element are shown in Fig.1.
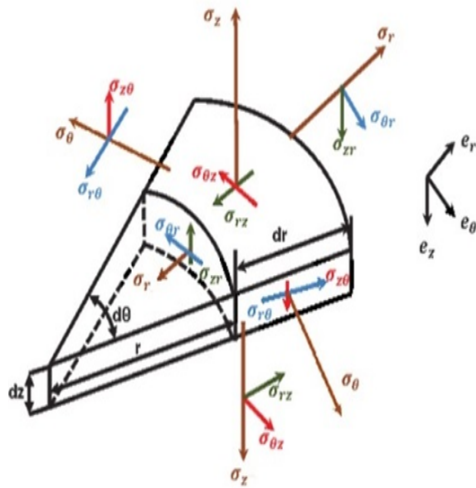


**Fig. 1A.** Cylindrical element of a transducer.

Since the transducer was excited longitudinally, and its designed natural mode was also longitudinal, shear stresses were negligible. Therefore the equations of motion along z and r directions are as follows:

$$\frac{\partial \sigma_r}{\sigma_r} + \frac{\sigma_r - \sigma_\theta}{r} = \rho \frac{\partial^2 U}{\partial t^2} \tag{A1}$$

$$\frac{\partial \sigma_z}{\partial z} = \rho \frac{\partial^2 U}{\partial t^2} \tag{A2}$$

By using relations between strain and displacements, the equations can be presented in terms of longitudinal and radial displacements. According to Poisson effect, there is a relationship between longitudinal and lateral stresses. The relation is modeled using the mechanical coupling coefficient, $n$, as follows [10].

$$n = \frac{\sigma_z}{\sigma_r + \sigma_\theta} \tag{A3}$$

Using the relations between stresses and strains (Hooke's Law) and also the mechanical coupling coefficient, normal strains in the cylindrical coordinate can be presented as follows:

$$S_r = \frac{1}{2}\left[\frac{1 - \nu - 2\nu n}{E}(\sigma_r + \sigma_\theta) + \frac{1+\nu}{E}(\sigma_r - \sigma_\theta)\right] \tag{A4}$$

$$S_\theta = \frac{1}{2}\left[\frac{1 - \nu - 2\nu n}{E}(\sigma_r + \sigma_\theta) - \frac{1+\nu}{E}(\sigma_r - \sigma_\theta)\right] \tag{A5}$$

$$S_z = \frac{1 - \dfrac{\nu}{n}}{E}[\sigma_z] \tag{A6}$$

In the above equations, $S_r$, $S_\theta$ and $S_z$ are normal strains along radial, circumferential and longitudinal directions, respectively. It is possible to obtain appropriate formulation for $\sigma_r$ and $(\sigma_r - \sigma_\theta)$ using Eqs. (A4) and (A5).

$$\sigma_r = \frac{E}{2}\left[\frac{S_r - S_\theta}{1+\nu} + \frac{S_r + S_\theta}{1 - \nu - 2\nu n}\right] \tag{A7}$$

$$\sigma_r - \sigma_\theta = \frac{E}{1+\nu}[S_r - S_\theta] \tag{A8}$$

### A.2. Apparent Wave Number and Elasticity Modulus of a Cylinder

Longitudinal differential equation of motion is as follows.

$$E_z \frac{\partial^2 U_z}{\partial z^2} = \rho \frac{\partial^2 U_z}{\partial t^2} \tag{A9}$$

where $E_z$ is apparent longitudinal elasticity modulus which define as follows:

$$E_z = \frac{E}{1 - \dfrac{\nu}{n}} \tag{A10}$$

In Eq. (A9), $U_z$ can be assumed as $U_z(z,t) = u_z(z)e^{iwt}$. Therefore, the differential equation can be presented as follows:

$$-u_z = \frac{\nu_z^2}{w^2}\left(\frac{\partial^2 u_z}{\partial z^2}\right) \tag{A11}$$

where $\nu_z = \sqrt{\dfrac{E_z}{\rho}}$ is the apparent longitudinal sound velocity. The apparent longitudinal wave number is defined as:

$$k_z = \frac{w}{\nu_z} \tag{A12}$$

Hence, the spatial part of the longitudinal differential equation is:

$$\frac{\partial^2 U_Z}{\partial z^2} + k_z^2 u_z = 0 \tag{A13}$$

The analytical solution of the equation is as follow:

$$u_z(z) = A\sin(k_z z) + B\cos(k_z z) \qquad (A14)$$

A and B are obtained by boundary conditions.

### A.3. Radial Frequency Equation of a Hollow Cylinder

Spatial part of the differential equation of motion along r direction is as follows:

$$\frac{\partial^2 u_r}{\partial r^2} + \frac{\partial u_r}{r\partial r} + \left(k_r^2 - \frac{1}{r^2}\right)u_r = 0 \qquad (A15)$$

where, $k_r = \dfrac{w}{\nu_r}$ is the apparent radial wave number, and $\nu_r = \sqrt{\dfrac{E_r}{\rho}}$ is apparent radial wave velocity. $E_r$ is apparent radial elastic modulus and expressed as:

$$E_r = \frac{E(1-\nu n)}{(1+\nu)(1-\nu-2\nu n)} \qquad (A16)$$

The analytical solution of the equation is as follows:

$$u_r(r) = C_1 J_1(k_r r) + C_2 Y_1(k_r r) \qquad (A17)$$

where, $J_1$ is the first order, first type Bessel function and $Y_1$ is the first order, second type Bessel function. Constant $C_1$ and $C_2$ are achieved by applying boundary conditions of a hollow vibrating cylinder. The boundary conditions of a free-free hollow cylinder are zero radial stresses at the internal and external radiuses. The following equations are achieved through applying boundary conditions at radius $b$, $a$.

$$C_1 j(a) + C_2 y(a) = 0 \qquad (A18)$$

$$C_1 j(b) + C_2 y(b) = 0 \qquad (A19)$$

To simplify the equations, the functions $y(x)$ and $j(x)$ are defined as:

$$j(x) = \left[k_r J_0(k_r x) - 2\frac{J_1(k_r x)}{x}\right](1-\nu-2\nu n)$$

$$+ (1+\nu)k_r J_0(k_r x) \qquad (A20)$$

$$y(x) = \left[k_r Y_0(k_r x) - 2\frac{Y_1(k_r x)}{x}\right](1-\nu-2\nu n)$$

$$+ (1+\nu)k_r Y_0(k_r x) \qquad (A21)$$

The Eqs. (A18) and (A19) are simplified as follows:

$$\frac{j(a)}{j(b)} = \frac{y(a)}{y(b)}$$

The radial frequency equation for a hollow cylinder would be expressed as:

$$\frac{k_r a J_0(k_r a) - \dfrac{(1-\nu-2\nu n)}{(1-\nu n)}(J_1(k_r a))}{k_r b J_0(k_r b) - \dfrac{(1-\nu-2\nu n)}{(1-\nu n)}(J_1(k_r b))} =$$

$$\frac{k_r a Y_0(k_r a) - \dfrac{(1-\nu-2\nu n)}{(1-\nu n)}(Y_1(k_r a))}{k_r b Y_0(k_r b) - \dfrac{(1-\nu-2\nu n)}{(1-\nu n)}(Y_1(k_r b))} \qquad (A23)$$

### A.4. Radial Frequency Equation of a Solid Cylinder

Two boundary conditions of a vibrating solid cylinder were zero radial stress at the external radius, and zero radial displacement at the center of the cylinder $u_r(r = 0) = 0$. Using the boundary conditions, the radial frequency equation would be as following:

$$ak_r J_0(k_r a) - \left[\frac{(1-\nu-2\nu n)}{(1-\nu n)}\right]J_1(k_r a) = 0 \qquad (A24)$$

### A.5. Radial Frequency Eequations of Piezoelectric Rings

Radial differential equation of a piezoelectric element, regardless of the shear strain, would be the same as Eq. (A1). If the axes 1, 2 and 3 in the Cartesian coordinate system will convert into $r$, $\theta$, $z$ in the cylindrical coordinate system, strain $S_r$, $S_\theta$, $S_z$ could be achieved using piezoelectric matrix equations as follows [16]:

$$S_r = S_{11}^E T_r + S_{12}^E T_\theta + S_{13}^E T_z \qquad (A25)$$

$$S_\theta = S_{21}^E T_r + S_{22}^E T_\theta + S_{23}^E T_z \qquad (A26)$$

$$S_z = S_{31}^E T_r + S_{32}^E T_\theta + S_{33}^E T_z \qquad (A27)$$

where $s_{ij}^E$ and $T_i$ are piezoelectric the compliance tensor in constant electric field, and the stress vector, respectively. In the strain equations of the piezoelectric, the effect of electrical field is ignored. In other words, the free vibration of the piezoelectric is taken into account in the zero electrical field. The mechanical coupling coefficient of piezoelectric is defined as $n = \dfrac{T_z}{T_r + T_\theta}$. Combining the mechanical coupling coefficient and the Eqs. (A25) through (A27), the following equations

would be achieved:

$$S_r + S_\theta = (S_{11}^E + S_{12}^E)(T_r + T_\theta) + 2S_{13}^E T_z$$

$$= (S_{11}^E + S_{12}^E + 2S_{13}^E n)(T_r + T_\theta) \tag{A28}$$

$$S_r - S_\theta = (S_{11}^E - S_{12}^E)(T_r - T_\theta) \tag{A29}$$

$$S_z = S_{13}^E(T_r + T_\theta) + S_{33}^E T_z = T_z\left(S_{33}^E + \frac{S_{13}^E}{n}\right) \tag{A30}$$

In the above equations, the piezoelectric compliance matrix symmetry has been used. The following equation for stress can be achieved from Eqs. (A28) and (A29).

$$T_r + T_\theta = \frac{1}{S_{11}^E + S_{12}^E + 2S_{13}^E n}(S_r + S_\theta) \tag{A31}$$

$$T_r - T_\theta = \frac{1}{S_{11}^E - S_{12}^E}(S_r - S_\theta) \tag{A32}$$

$$T_r = \frac{1}{2}\left[\frac{1}{S_{11}^E - S_{12}^E}(S_r - S_\theta)\right.$$

$$\left. + \frac{1}{S_{11}^E + S_{12}^E + 2S_{13}^E n}(S_r + S_\theta)\right] \tag{A33}$$

Radial differential equation of piezoelectric would be as:

$$\frac{\partial^2 u_r}{\partial r^2} + \frac{1}{r}\frac{\partial u_r}{\partial r} + \left(k_r^2 - \frac{1}{r^2}\right)u_r = 0 \tag{A34}$$

where, the apparent radial elastic modulus, sound velocity and wave number are defined as follows:

$$E_r = \frac{S_{11}^E + S_{13}^E n}{(S_{11}^E - S_{12}^E)(S_{11}^E + S_{12}^E + 2S_{13}^E n)} \tag{A35}$$

$$v_r = \sqrt{\frac{E_r}{\rho}} \tag{A36}$$

$$k_r = \frac{w}{\rho\sqrt{\frac{S_{11}^E + S_{13}^E n}{(S_{11}^E - S_{12}^E)(S_{11}^E + S_{12}^E + 2S_{13}^E n)}}} \tag{A37}$$

Analytical solution of Eq. (A.34) would be as:

$$u_r(r) = D_1 J_1(k_r r) + D_2 Y_1(k_r r)$$

Using the free vibration boundary conditions of a piezoelectric ring, i.e. zero stress at the internal and external radiuses, the radial frequency equation is achieved as:

$$\frac{k_r a J_0(k_r a) - \left[\frac{(S_{11}^E + S_{12}^E + 2nS_{13}^E)}{(S_{11}^E + nS_{13}^E)}\right] J_1(k_r a)}{k_r b J_0(k_r b) - \left[\frac{(S_{11}^E + S_{12}^E + 2nS_{13}^E)}{(S_{11}^E + nS_{13}^E)}\right] J_1(k_r b)} =$$

$$\frac{k_r a Y_0(k_r a) - \left[\frac{(S_{11}^E + S_{12}^E + 2nS_{13}^E)}{(S_{11}^E + nS_{13}^E)}\right] Y_1(k_r a)}{k_r b Y_0(k_r b) - \left[\frac{(S_{11}^E + S_{12}^E + 2nS_{13}^E)}{(S_{11}^E + nS_{13}^E)}\right] Y_1(k_r b)} \tag{A39}$$

Spatial part of the longitudinal differential equation of the piezoelectric is as follow:

$$\frac{\partial^2 u_z}{\partial z^2} + k_z^2 u_z = 0 \tag{A40}$$

where, $k_z$ piezoelectric apparent wave number is defined as:

$$k_z = \frac{w}{\sqrt{\frac{1}{\left(S_{33}^E + \frac{S_{13}^E}{n}\right)}}} \tag{A41}$$

The apparent longitudinal elastic modulus is defined as:

$$E_z = \frac{1}{\rho\left(S_{33}^E + \frac{S_{13}^E}{n}\right)} \tag{A42}$$

# References

[1] U.S. Bhirud, P.R. Gogate, A.M. Wilhelm, A.B. Panlit, Ultrasonic bath with longitudinal vibrations: A novel configuration for efficient wastewater treatment, Ultrason. Sonochem., 11(3-4) (2004) 143-147.

[2] B. Verhaagen, T. Zanderink, D.F. Rivas, Ultrasonic cleaning of 3D printed objects and Cleaning Challenge Devices, Appl. Acoust., 10 (2016) 172-181.

[3] A. Benatar, Ultrasonic welding of plastics and polymeric composites, Power Ultrasonics, Woodhead Publisher, (2015).

[4] S. Elangovan, K. Prakasan, V. Jaiganesh, Optimization of ultrasonic welding parameters for copper to copper joints using design of experiments, Int. J. Adv. Manuf. Tech., 51(1-4) (2010) 163-171.

[5] T.B. Thoe, D.K. Aspinwall, M.L.H. Wise, Review on ultrasonic machining, Int. J. Mach. Tools Manuf., 38(4) (1998) 239-255.

[6] S. Bagherzadeh, K. Abrinia, Q. Han, Ultrasonic assisted equal channel angular extrusion (UAE) as a novel hybrid method for continuous production of ultra-fine grained metals, Mater. Lett., 169(5) (2016) 90-94.

[7] A. Abdullah, M. Shahini, A. Pak, An approach to design a high power piezoelectric ultrasonic transducer, J. Electroceram., 22(4) (2006) 369-382.

[8] R. Mahdavinejad, Finite element dimensional design and modeling of an ultrasonic transducer, J. Sci. Technol., 29(B2) (2005) 253-263.

[9] R. Lerch, Simulation of piezoelectric devices by two and three-dimensional finite elements, IEEE T. Ultrason. Ferr. Cont., 37(3) (1990) 233-247.

[10] E. Mori, K. Itoh, A. Imamura, Analysis of a short column vibrator by apparent elasticity method and its application, ultrasonics international conference proceedings, (1977) 262-265.

[11] E. Mori, K. Yamakoshi, Coupled vibration of a cylindrical shell for radiating high intensity ultrasound, Ultrasonics, 16(2) (1987) 81-83.

[12] Y. Watababe, Y. Tsuda, E. Mori, A study on directional converter for ultrasonic longitudinal mode vibration by using a hollow cylinder type resonator, ultrasonic international conference proceeding, (1993) 495-498.

[13] L. Shuyu, Design of piezoelectric sandwich ultrasonic transducers with large cross-section, Appl. Acoust., 44(3) (1995) 249-257.

[14] D. Dragan, R. Milan, Design of ultrasonic transducers by means of the apparent elasticity method, Facta Universitatis, 2(4) (2004) 293-300.

[15] G.P. Zhou, M.J. Liang, The vibration behavior and design of langevin transducer with radial coupling, J. Sound. Vib., 220(48) (2003) 29-32.

[16] S.Y. Lin, Coupled vibration analysis of piezoelectric ceramic disk resonators, J. Sound. Vib., 218(2) (1998) 205-217.

[17] S.Y. Lin, Coupled vibration of isotropic metal hollow cylinders with large geometrical dimensions, J. Sound. Vib., 305(1-2) (2007) 308-316.

[18] A. Abdollah, M. Shahini, A. Pak, An approach to design a high power piezoelectric ultrasonic transducer, J. Electroceram, (22) (2009) 369-382.